DMD Fast Forward. Published on May 11, 2018 as DOI: 10.1124/dmd.117.079640
This article has not been copyedited and formatted. The final version may differ from this version.

Multidrug Resistance Protein 1 (MRP1/*ABCC1*)-mediated cellular protection and transport of methylated arsenic metabolites differs between human cell lines.

Mayukh Banerjee, Gurnit Kaur, Brayden D. Whitlock, Michael W. Carew, X. Chris Le, and Elaine M. Leslie

Department of Physiology (*MB, BDW, MWC, EML*), Membrane Protein Disease Research Group (*MB, GK, BDW, MWC, EML*), and Department of Laboratory Medicine and Pathology (*GK, XCL,EML*) University of Alberta, Edmonton, AB, Canada.

DMD Fast Forward. Published on May 11, 2018 as DOI: 10.1124/dmd.117.079640
This article has not been copyedited and formatted. The final version may differ from this version.

Running Title: MRP1 transport of methylated arsenic species

Corresponding author: Elaine M. Leslie, Department of Physiology, 7-08A Medical Sciences Building, University of Alberta, Edmonton, AB, Canada, Tel.: (780) 492 9250; Fax: (780) 248 1995; email: eleslie@ualberta.ca.

Text pages: 25

Tables: 2

Figures: 5

Supplemental Figures: 2

References: 70

Abstract: 249 words

Introduction: 754 words

Discussion: 1948

Non-standard abbreviations: ABC, ATP-binding cassette; As^{V}, arsenate; As^{III}, arsenite; $As(GS)_3$, arsenic triglutathione; DMA^{III}, dimethylarsinous acid; DMA^{V}, dimethylarsinic acid; $E_2 17\beta G$, 17β-estradiol 17-(β-D-glucuronide); HEK293, human embryonic kidney 293; IC_{50}, half-maximal inhibitory concentration; ICP-MS, inductively coupled plasma mass spectrometry; K_i, inhibitor constant; K_M, Michaelis constant; LTC_4, leukotriene C_4; MMA^{III}, monomethylarsonous acid; MMA^{V}, monomethylarsonic acid; $MMA(GS)_2$, monomethylarsenic diglutathione; MRP, multidrug resistance protein; MSD, membrane spanning domain; NBD, nucleotide binding domain; PIC, phosphatase inhibitor cocktail; WT, wild-type.

DMD Fast Forward. Published on May 11, 2018 as DOI: 10.1124/dmd.117.079640
This article has not been copyedited and formatted. The final version may differ from this version.

Abstract

The ATP-binding cassette (ABC) transporter Multidrug Resistance Protein 1 (MRP1/*ABCC1*) protects cells from arsenic (a proven human carcinogen), through the cellular efflux of arsenic triglutathione [$As(GS)_3$], and the diglutathione conjugate of monomethylarsonous acid (MMA^{III}) [$MMA(GS)_2$]. Previously, differences in MRP1 phosphorylation (at Y920/S921) and *N*-glycosylation (at N19/N23) were associated with marked differences in $As(GS)_3$ transport kinetics between HEK293 and HeLa cell lines. In the current study, cell line differences in MRP1-mediated cellular protection, and transport of other arsenic metabolites, were explored. MRP1 expressed in HEK293 cells reduced the toxicity of the major urinary arsenic metabolite dimethylarsinic acid (DMA^V), and HEK-WT-MRP1-enriched vesicles transported DMA^V with high apparent affinity and capacity (K_m 0.19 µM, V_{max} 342 pmol mg^{-1} protein min^{-1}). This is the first report that MRP1 is capable of exporting DMA^V, critical for preventing highly toxic dimethylarsinous acid (DMA^{III}) formation. In contrast, DMA^V transport was not detected using HeLa-WT-MRP1 membrane vesicles. $MMA(GS)_2$ transport by HeLa-WT-MRP1 vesicles had a greater than 3-fold higher V_{max}, compared to HEK-WT-MRP1 vesicles. Cell line differences in DMA^V and $MMA(GS)_2$ transport were not explained by differences in phosphorylation at Y920/S921. DMA^V did not inhibit, while $MMA(GS)_2$ was an uncompetitive inhibitor of $As(GS)_3$ transport, suggesting that DMA^V and $MMA(GS)_2$ have non-identical binding sites to $As(GS)_3$ on MRP1. Efflux of different arsenic metabolites by MRP1 is likely influenced by multiple factors including cell and tissue type. This could have implications for the impact of MRP1 on both tissue specific susceptibility to arsenic-induced disease, and tumour sensitivity to arsenic-based therapeutics.

DMD Fast Forward. Published on May 11, 2018 as DOI: 10.1124/dmd.117.079640
This article has not been copyedited and formatted. The final version may differ from this version.

Introduction

Arsenic is a proven human carcinogen, causing lung, skin, and bladder tumors (IARC, 2012). Chronic arsenic exposure is associated with increased incidences of kidney and liver tumors, and a myriad of non-cancerous adverse health effects (Platanias, 2009; IARC, 2012; Naujokas et al., 2013). Millions of people world-wide are exposed to levels of arsenic above the World Health Organization acceptable level of 10 μg/l, predominantly through the consumption of groundwater naturally contaminated with inorganic arsenic [arsenite (As^{III}) and arsenate (As^{V})] (Rahman et al., 2009). In addition to environmental exposures, arsenic trioxide is used clinically in the treatment of acute promyelocytic leukemia and is in clinical trials for the treatment of other hematological and solid tumors (Kritharis et al., 2013; Ally et al., 2016; Cicconi and Lo-Coco, 2016; Falchi et al., 2016). Other arsenic compounds are also in clinical trials for the treatment of various cancers (Khairul et al., 2017). Thus, understanding the cellular handling of arsenic is critical for the development of therapeutics to treat chronic arsenic exposure, and to maximize the clinical effectiveness of arsenic based drugs.

Cellular uptake of arsenic has been recently reviewed (Mukhopadhyay et al., 2014; Roggenbeck et al., 2016). Once inside most mammalian cells, arsenic undergoes extensive methylation (Vahter, 1999; Drobna et al., 2010). In humans, the four major methylation products are monomethylarsonic acid (MMA^{V}), monomethylarsonous acid (MMA^{III}), dimethylarsinic acid (DMA^{V}), and dimethylarsinous acid (DMA^{III}) (Thomas et al., 2007). Arsenic methylation has a significant impact on its toxicity, tissue distribution, and retention (Thomas et al., 2004; Thomas et al., 2007; Wang et al., 2015). Although arsenic methylation results in an increased rate of arsenic whole body clearance (Drobna et al., 2009; Drobna et al., 2010; Hughes et al., 2010), and reduces susceptibility to acute arsenic toxicity (Yokohira et al., 2010; Yokohira et al., 2011), trivalent methylated forms of arsenic (MMA^{III} and

DMD Fast Forward. Published on May 11, 2018 as DOI: 10.1124/dmd.117.079640
This article has not been copyedited and formatted. The final version may differ from this version.

DMA^{III}) are considered bioactivation products because they are more reactive metabolites than As^{III} (Petrick et al., 2000; Styblo et al., 2000; Mass et al., 2001; Kligerman et al., 2003; Moe et al., 2016).

In addition to methylation, arsenic can be conjugated with reduced glutathione (GSH/GS) (Leslie, 2012). Arsenic triglutathione [$As(GS)_3$] and the diglutathione conjugate of the highly toxic MMA^{III} [$MMA(GS)_2$], have been isolated from rat bile and mouse urine, thus, these two As-GSH complexes are formed physiologically, and account for a major fraction of arsenic in urine and bile (Kala et al., 2000; Suzuki et al., 2001; Cui et al., 2004; Kala et al., 2004; Bu et al., 2011). The ATP-binding cassette (ABC) transporter Multidrug Resistance Protein 1 (MRP1, gene symbol *ABCC1*), along with the related MRP2 and MRP4 (*ABCC2* and *ABCC4,* respectively) mediate the cellular export of multiple methylated and/or glutathionylated metabolites of arsenic (Kala et al., 2000; Kala et al., 2004; Leslie et al., 2004; Carew and Leslie, 2010; Carew et al., 2011; Banerjee et al., 2014; Shukalek et al., 2016).

MRP1 is a 190 kDa phosphoglycoprotein with three polytopic membrane spanning domains (MSDs) and two nucleotide binding domains (NBDs) arranged as MSD0-MSD1-NBD1-MSD2-NBD2 (Cole, 2014). MRP1 confers resistance to a chemically diverse array of anti-cancer drugs and is involved in the cellular export of physiological compounds including GSH, glutathione disulphide, 17β-estradiol 17-(β-D-glucuronide) ($E_217\beta G$), and leukotriene C_4 (LTC_4) (Cole, 2014). Furthermore, MRP1 transports a variety of xenobiotics often conjugated to GSH, glucuronate, or sulphate (Jedlitschky et al., 1996; Loe et al., 1996a; Loe et al., 1996b; Leslie et al., 2005). Included in this list are the arsenic metabolites $As(GS)_3$ and $MMA(GS)_2$, the glutathionylated forms of inorganic arsenic (As^{III} and As^V) and MMA^{III}, respectively (Leslie et al., 2004; Carew et al., 2011).

Interestingly, $As(GS)_3$ is transported by MRP1 expressed in HEK293 cells with

DMD Fast Forward. Published on May 11, 2018 as DOI: 10.1124/dmd.117.079640
This article has not been copyedited and formatted. The final version may differ from this version.

markedly different kinetics than by MRP1 expressed in HeLa cells (Shukalek et al., 2016). Further investigation revealed that MRP1 affinity and capacity for $As(GS)_3$ was associated with the phosphorylation status of two residues in the linker region between NBD1 and MSD2 (Y920 and S921). Furthermore, the glycosylation status of two residues in the amino-terminus (N19 and N23) influenced the stability of Y920 and/or S921 phosphorylation (Shukalek et al., 2016). Given this cell line difference, the first objective of the current study was to determine differences in arsenical cytotoxicity between the HEK-MRP1 and HeLa-MRP1 cell lines. The second objective was to use MRP1-enriched membrane vesicles isolated from HEK and HeLa cells to determine the cell line differences in MRP1 transport function. The third objective was to investigate the influence of Y920/S921 phosphorylation on the ability of HEK-MRP1-enriched membrane vesicles to transport arsenic metabolites in addition to $As(GS)_3$.

DMD Fast Forward. Published on May 11, 2018 as DOI: 10.1124/dmd.117.079640
This article has not been copyedited and formatted. The final version may differ from this version.

Materials and Methods

Materials: Carrier-free $^{73}As^{V}$ (158 Ci/mol) was purchased from Los Alamos Meson Production Facility (Los Alamos, NM). Tris base, GSH, ATP, AMP, sucrose, DMA^{V} (>99% purity), $MgCl_2$, creatine kinase, GSH reductase, creatine phosphate, NADPH, sodium (meta)-arsenite [Na_2AsO_2] (>99% pure), As^{V} (>98% purity), sodium metabisulfite [$Na_2S_2O_5$], and sodium thiosulfate [$Na_2S_2O_3$] were from Sigma-Aldrich (Oakville, Canada). Protease inhibitor cocktail tablets (Complete, Mini, EDTA-free) and PhosSTOP phosphatase inhibitor cocktail (PIC) tablets were purchased from Roche Applied Science (Laval, Canada). Phenylmethylsulfonyl fluoride was from Bioshop Canada Inc. (Burlington, Canada). Suprapur® nitric acid was purchased from Merck (Darmstadt, Germany). MMA^{III} and DMA^{III} in the form diiodomethylarsine (CH_3AsI_2) and iododimethylarsine ($[CH_3]_2AsI$), respectively, were synthesized as previously described (Cullen et al., 2016), and were at least 99% pure as confirmed by NMR analysis. The rat monoclonal antibody (mAb) MRPr1 was from Novus Biologicals (Littleton, CO), while rabbit anti-Na^{+}/K^{+}ATPase (H-300) was purchased from Santa Cruz Biotechnology, Inc. (Santa Cruz, CA).

Cell lines and stable transfection: HEK293T cells were obtained from the American Type Culture Collection (Rockville, MD) and maintained in Dulbecco's modified Eagle's medium (DMEM) with 7.5% fetal bovine serum. HeLa and HEK293 cell lines stably expressing the empty pcDNA3.1(-) vector (HeLa-vector) and/or pcDNA3.1(-)-MRP1 (HeLa-MRP1 and HEK-MRP1) were gifts from Dr. Susan P.C. Cole (Queen's University, Kingston, Canada) and generated as described previously (Ito et al., 2001; Conseil and Cole, 2013). The HEK-vector expressing cell line (HEK-V4) was generated as described previously (Banerjee et al., 2014). HeLa stables were maintained in Roswell Park Memorial Institute (RPMI)-1640 medium with 5% calf serum and 600 µg/ml G418 (Geneticin). HEK293 stables were maintained in DMEM with 7.5% fetal bovine serum and 600 µg/ml G418. Stable cell

DMD Fast Forward. Published on May 11, 2018 as DOI: 10.1124/dmd.117.079640
This article has not been copyedited and formatted. The final version may differ from this version.

lines were checked for the proportion of cells expressing MRP1 by flow cytometry (BD FACS Calibur, Cross Cancer Institute) using the MRP1-specific MAb MRPr1, as described previously (Hipfner et al., 1994; Leslie et al., 2003). Populations of less than 80% were not used in experiments.

Cytotoxicity Testing: The cytotoxicity of five arsenic species was measured using HEK-vector, HEK-MRP1, HeLa-vector, and HeLa-MRP1 as previously described (Carew et al., 2011). Briefly, cells were seeded in 96-well plates at 1 x 10^4 cells/well and grown for 24 h. In quadruplicate, cells were treated with As^{III} (0.01-300 μM), As^{V} (0.05-5000 μM), MMA^{III} (0.03-30μM), DMA^{III} (0.01-300 μM), or DMA^{V} (0.01-30 mM) for 72 h. These doses were experimentally determined to range from non-toxic to causing complete loss of viability over 72 h. The pH of DMA^{V} was adjusted to pH 7.4 prior to treating cells. Cytotoxicity was determined using the tetrazolium-based MTS assay [CellTiter 96 Aqueous Non-Radioactive Cell Proliferation Assay (Promega, Madison, WI)], according to the manufacturer's instructions. The IC_{50}, defined as the concentration of arsenical that resulted in half the maximal toxic effect, for each arsenical, was determined for HEK-MRP1 and HEK-vector cells using the sigmoidal dose-response equation in GraphPad Prism (GraphPad Software, La Jolla, CA). Relative resistance values (equivalent to relative protection), defined as the ratio of the IC_{50} value in HEK-MRP1 to that in HEK-vector, were determined for each arsenical tested.

Site-Directed Mutagenesis: Mutants of MRP1 (S905A-, S915A-, S916A-, S917A-, Y920F-, S921A-, Y920F/S921A-, Y920E/S921E-, and T931A-MRP1) were generated previously (Shukalek et al., 2016). In addition, several new potential phosphorylation mutants (S916E-, S918A-, S919A-, and S919E-MRP1) were generated using the QuikChange II XL site-directed mutagenesis kit (Stratagene, Agilent Technologies, Santa Clara, CA). pcDNA3.1(-)-MRP1 was used as the PCR template and mutagenesis was carried out according to the manufacturer's instructions using mutagenic primers from Integrated DNA Technology (Coralville, IA), sequences are available upon request. The incorporation of desired mutations was confirmed by DNA sequencing (Molecular Biology Servicing Unit, University of Alberta, Edmonton, Canada).

Expression of wild-type (WT) and mutant forms of MRP1 in HEK293T cells, preparation of membrane vesicles, and immunoblots: HEK293T cells were transfected using the calcium-phosphate method as described previously (Carew and Leslie, 2010), and incubated for 48–72 h post-transfection. For membrane vesicle preparations, WT and MRP1 mutant-transfected cells were collected by centrifugation, layered with Tris sucrose buffer (50 mM Tris, pH 7.4, 250 mM sucrose) containing $CaCl_2$ (0.25 mM), EDTA-free protease inhibitors, and where indicated, phosSTOP PIC, and cell pellets stored at -80°C until plasma membrane-enriched vesicles were isolated as described previously (Carew and Leslie, 2010). Expression of WT and MRP1 mutants were confirmed by immunoblotting as described previously (Shukalek et al., 2016), using the MRPr1 antibody (1:10,000 dilution). Blots were also probed for Na^+/K^+-ATPase as a loading control using the Na^+/K^+-ATPase specific antibody H-300 (1:10,000 dilution), except in the case of comparison of MRP1 levels between the two different cell lines (the Na^+/K^+-ATPase level was found to be different). Thus, blots were stained with Coomassie blue and normalized to total protein levels in each lane. Relative levels of MRP1 were quantified using ImageJ Software (National Institutes of Health, Bethesda, MD) and/or ImageLab Software (Bio-Rad, Hercules, CA).

$MMA(GS)_2$, DMA^V, and $As(GS)_3$ vesicular transport assays: Reduction of arsenate [$^{73}As^V$] into arsenite [$^{73}As^{III}$] and subsequent synthesis of $^{73}As(GS)_3$ from $^{73}As^{III}$ and GSH, were carried out as described previously (Reay and Asher, 1977; Shukalek et al., 2016). $MMA(GS)_2$ was synthesized from MMA^{III} and GSH as described previously (Carew et al., 2011; Banerjee et al., 2014). Vesicular transport was carried out in triplicate for each

DMD Fast Forward. Published on May 11, 2018 as DOI: 10.1124/dmd.117.079640
This article has not been copyedited and formatted. The final version may differ from this version.

substrate, employing previously described methods (Carew et al., 2011; Banerjee et al., 2014; Shukalek et al., 2016). The amount of ^{73}As(GS)$_3$ transported was quantified using liquid scintillation counting, as described previously (Leslie et al., 2004; Shukalek et al., 2016). The amount of MMA(GS)$_2$ and DMA^V transported was quantified by inductively coupled plasma mass spectrometry (ICP-MS) using the standard addition method, as described previously (Banerjee et al., 2014). ATP-dependent transport was calculated by subtracting transport in the presence of AMP from transport in the presence of ATP, and data expressed as pmol or nmol As(GS)$_3$, MMA(GS)$_2$ or DMA^V transported mg^{-1} protein min^{-1}.

The linear range of DMA^V transport was determined by incubating the HEK-WT-MRP1 or HEK-vector membrane vesicles with DMA^V (1µM) in transport buffer at 37°C for the indicated time points. Kinetic parameters were determined by measuring the initial rate of DMA^V and MMA(GS)$_2$ transport at eight different substrate concentrations [0.1–2.5 µM for DMA^V and 1–200 µM for MMA(GS)$_2$] at 20 sec and 1 min, respectively. Curve fitting was done by nonlinear regression analysis using GraphPad Prism® 6 software (La Jolla, CA).

The ability of DMA^V and MMA(GS)$_2$ to inhibit ^{73}As(GS)$_3$ transport was first characterized by using a fixed concentration of ^{73}As(GS)$_3$ (1 µM, 40 nCi) in the presence of increasing concentrations of DMA^V (0.04 and 1000 µM) or MMA(GS)$_2$ (0.01-300 µM). The conditions for the synthesis of As(GS)$_3$ resulted in the presence of 3 mM GSH in transport reactions (Leslie et al., 2004). Thus, As(GS)$_3$ inhibition experiments were completed under plus GSH conditions. This is important because the *in vitro* inhibition of MRP1 by certain compounds can be enhanced by physiological concentrations of GSH (Cole and Deeley, 2006). IC$_{50}$ values were calculated for MMA(GS)$_2$ inhibition using GraphPad Prism® 6 Software [nonlinear regression log(inhibitor) vs response variable slope (four parameters)]. To determine the mode of inhibition of ^{73}As(GS)$_3$ by MMA(GS)$_2$, the K_i of MMA(GS)$_2$ was determined by performing ^{73}As(GS)$_3$ (0.1-20 µM, 40-100 nCi) transport in the presence of

DMD Fast Forward. Published on May 11, 2018 as DOI: 10.1124/dmd.117.079640
This article has not been copyedited and formatted. The final version may differ from this version.

three different $MMA(GS)_2$ concentrations (5, 10, and 15 μM), as described previously (Leslie et al., 2004).

All transport data were normalized as needed to correct for any difference in level of HeLa-WT-MRP1 or mutant MRP1 expressed in HEK cells relative to HEK-WT-MRP1 as determined by immunoblotting of each membrane vesicle preparation. Positive control transport experiments using $MMA(GS)_2$ or $As(GS)_3$ were run for each vesicle preparation, as described above and previously (Leslie et al., 2004; Carew et al., 2011).

DMD Fast Forward. Published on May 11, 2018 as DOI: 10.1124/dmd.117.079640
This article has not been copyedited and formatted. The final version may differ from this version.

Results

MRP1 expressed in HEK293 cells decreases the cytotoxicity of As^{III}, As^{V}, MMA^{III}, and DMA^{V}. Previously we have shown that MRP1 stably expressed in HeLa cells reduced the toxicity of As^{III}, As^{V}, and MMA^{III}, but not MMA^{V}, DMA^{III}, or DMA^{V} relative to HeLa cells expressing empty vector alone (Carew et al., 2011). Given that we have recently reported substantial differences in the transport of $As(GS)_3$ between MRP1-enriched membrane vesicles isolated from HEK293 and HeLa cells (Shukalek et al., 2016), differences in arsenical cytotoxicity between the two cell lines were investigated. Thus, the cytotoxicity of five of these arsenicals (As^{III}, As^{V}, MMA^{III}, DMA^{III}, and DMA^{V}) in HEK-MRP1 and HEK-vector cell lines were determined in parallel with HeLa-MRP1 and HeLa-vector for comparison [Figure 1, Table 1, and (Carew et al., 2011)].

The arsenic compounds that HEK-MRP1 cells conferred resistance to (relative to HEK-vector) were the same as the HeLa cell line pair (Figure 1A-C and Table 1), except that HEK-MRP1 conferred a significantly increased level of resistance against DMA^{V} (relative resistance value of 1.4, $P < 0.05$) [Figure 1D, Table 1, and (Carew et al., 2011)]. In addition, HEK-MRP1 cells had a relative resistance of 9.2 against As^{V} (Table 1 and Figure 1B), while HeLa-MRP1 cells had a relative resistance of only 2.1 [Table 1 and (Carew et al., 2011)]. These results led us to characterize the cell line differences for DMA^{V} and As^{V} transport using MRP1-enriched membrane vesicles. Furthermore, although resistance to MMA^{III} was conferred by both HEK-MRP1 and HeLa-MRP1 cell lines [Figure 1C, Table 1 and (Carew et al., 2011)], differences in transport characteristics between membrane vesicles prepared from these cell lines were also investigated for $MMA(GS)_2$.

Transport of DMA^{V} by MRP1-enriched membrane vesicles: To test if differences in cytotoxicity were due at least in part to differences in ATP-dependent cellular efflux, DMA^{V} transport by HEK- and HeLa-WT-MRP1 membrane vesicles was measured at 0.05

DMD Fast Forward. Published on May 11, 2018 as DOI: 10.1124/dmd.117.079640
This article has not been copyedited and formatted. The final version may differ from this version.

and 1 μM of DMA^V (Figure 2A). MRP1-enriched vesicles prepared from transiently transfected HEK293T cells transported DMA^V (101 ± 15 pmol mg^{-1} protein min^{-1} at 0.05 μM and 264 ± 42 pmol mg^{-1} protein min^{-1} at 1 μM). In contrast, DMA^V transport was not detected for HeLa-WT-MRP1 vesicles (Figure 2A), despite the fact that the same vesicle preparations were functional for $MMA(GS)_2$ transport (Figure 4A), and comparable levels of MRP1 were present (Supplemental Figure 1). For certain compounds transported by MRP1, GSH can either be required for or enhance transport (Cole, 2014). To determine if this was the case for DMA^V, transport assays were completed in the presence of 3 mM GSH, and this had no effect on HEK- or HeLa-WT-MRP1 DMA^V transport activity (data not shown). Thus, we report for the first time that MRP1 is capable of transporting this important methylated arsenic metabolite, at least under certain conditions.

Kinetic analysis of MRP1-mediated DMA^V transport: Transport of DMA^V by HEK-WT-MRP1 membrane vesicles was then further characterized. The linear range of DMA^V (1 μM) transport versus time was measured for HEK-WT-MRP1 and HEK-vector control membrane vesicles (Figure 2B). Transport by HEK-WT-MRP1 was linear for up to 30 sec and reached a maximal activity of 138 ± 24 pmol mg^{-1} protein at 30 sec. ATP-dependent transport of DMA^V by HEK-vector was very low and similar to transport observed in the presence of AMP. HEK-WT-MRP1 membrane vesicle transport of DMA^V was characterized kinetically by determining the initial rates of transport over several concentrations of DMA^V (Figure 2C and Table 2). HEK-MRP1 was found to transport DMA^V with high apparent affinity and capacity (K_m of 0.19 ± 0.06 μM and V_{max} of 342 ± 37 pmol mg^{-1} protein min^{-1}).

Analysis of DMA^V transport by HEK-MRP1 phosphorylation mutants: Due to the complete lack of DMA^V transport by HeLa-WT-MRP1 and substantial transport by HEK-WT-MRP1 membrane vesicles, this cell line difference was further explored. We have

DMD Fast Forward. Published on May 11, 2018 as DOI: 10.1124/dmd.117.079640
This article has not been copyedited and formatted. The final version may differ from this version.

previously shown that HEK293 and HeLa cell line differences in $As(GS)_3$ transport by MRP1 were associated with differences in phosphorylation at Y920/S921 (Shukalek et al., 2016). In order to determine if phosphorylation differences at these sites were responsible for the difference in DMA^V transport by MRP1 between the two cell lines, DMA^V transport by MRP1-Y920/S921 dephosphorylation- and phosphorylation-mimicking mutants was investigated.

Dephosphorylation-mimicking HEK-Y920F/S921A-MRP1 membrane vesicles exhibited a complete loss of DMA^V transport (Figure 3A), suggesting these sites are critical for the cell line difference. However, the phosphorylation-mimicking HEK-Y920E/S921E-MRP1, which we expected would restore DMA^V transport, also completely lacked DMA^V transport (Figure 3A). Furthermore, individual dephosphorylation mimicking mutants Y920F-MRP1 and S921A-MRP1 also completely lost function (data not shown). Mutant membrane vesicle preparations had MRP1 levels similar to HEK-WT-MRP1 (Supplemental Figure 1), and were functional for $MMA(GS)_2$ (Figure 4B, Table 2) and/or $As(GS)_3$ (Supplementa1 Figure 2A) transport .

Analysis of DMA^V transport by HeLa-WT-MRP1 in the presence of phosphatase inhibitors: The possible modulation of DMA^V transport by MRP1 through phosphorylation was also investigated by studying the transport in MRP1-enriched vesicles prepared from HeLa cells in the presence or absence of a phosphatase inhibitor cocktail (PIC) at two different substrate concentrations (0.05 and 1 μM) (Figure 3B). We have previously shown for $As(GS)_3$ that HeLa-WT-MRP1 membrane vesicles prepared in the presence of a PIC have a 19- and 12-fold increase in K_m and V_{max}, respectively, compared to HeLa-WT-MRP1 prepared in the absence of a PIC (Shukalek et al., 2016). In contrast, the inclusion of a PIC did not influence DMA^V transport by HeLa-WT-MRP1 at either concentration (Figure 3B). To ensure that the HeLa-WT-MRP1 ± PIC membrane vesicles used in the DMA^V transport

DMD Fast Forward. Published on May 11, 2018 as DOI: 10.1124/dmd.117.079640
This article has not been copyedited and formatted. The final version may differ from this version.

assays were functional, and the PIC active, $As(GS)_3$ transport experiments were completed on the same vesicle preparations (Figure 3C). Consistent with our previous report (Shukalek et al., 2016), $As(GS)_3$ transport by HeLa-WT-MRP1 vesicles, prepared in the presence of a PIC, was significantly higher than for HeLa-WT-MRP1 vesicles prepared in the absence of a PIC. These results could suggest that mechanisms other than phosphorylation are likely responsible for the cell line difference observed in DMA^V transport by HEK-WT-MRP1 compared to HeLa-WT-MRP1. Alternatively, a differential phosphorylation site that remains stable in the absence of PIC could be involved.

The lack of DMA^V transport by all mutants of Y920/S921 could also be due to the disruption of phosphorylation/dephosphorylation of neighboring sites that are critical for DMA^V transport. We screened the influence of seven additional putative phosphorylation sites in the linker region (S905-, S915-, S916-, S917-, S918-, S919-, T931-MRP1) by mutating them to phospho-mimicking and/or dephospho-mimicking residues in full length MRP1, expressing them in HEK293 cells, preparing membrane vesicles, and measuring DMA^V transport. Surprisingly, all mutants lacked DMA^V transport activity, despite the fact that they were comparable to HEK-WT-MRP1 for $As(GS)_3$ transport and MRP1 level (Supplemental Figure 2).

Inhibition of $As(GS)_3$ transport by DMA^V: To further characterize the differences in interaction of $As(GS)_3$ and DMA^V with MRP1, transport of $As(GS)_3$ (1 μM) by HEK-WT-MRP1 vesicles was measured in the presence of DMA^V. DMA^V did not inhibit $As(GS)_3$ transport even at a concentration of 1 mM (data not shown), four orders of magnitude greater than the apparent K_m of DMA^V for MRP1 (Table 2).

MRP1 Does Not Transport As^V: Given the striking difference in As^V relative resistance levels between the HeLa and HEK293 cell line pairs [Figure 1B, Table 1 and (Carew et al., 2011)], the ability of HEK-MRP1 and HeLa-MRP1 membrane vesicles to

DMD Fast Forward. Published on May 11, 2018 as DOI: 10.1124/dmd.117.079640
This article has not been copyedited and formatted. The final version may differ from this version.

transport As^V was investigated. As^V (1 and 10 μM) was not transported by MRP1-enriched membrane vesicles prepared from HEK293 cells in the presence or absence of 3 mM GSH (data not shown). Similar results were obtained for membrane vesicles prepared from HeLa-MRP1 cells (data not shown). These results are consistent with a lack of detectable As^V transport (in the presence and absence of GSH) by MRP1-enriched vesicles prepared from the H69AR small cell lung cancer cell line, and our previous conclusion that inorganic arsenic (As^{III} and As^V) is metabolized to $As(GS)_3$ prior to transport by MRP1 (Leslie et al., 2004).

Transport of $MMA(GS)_2$ by MRP1-enriched membrane vesicles: We have previously shown that MMA^{III} is transported by HEK-MRP1 in the form $MMA(GS)_2$ and that HeLa-MRP1 cells confer protection against MMA^{III} relative to HeLa-vector cells (Carew et al., 2011). In the current study, HEK-MRP1 cells were also found to confer protection against MMA^{III} relative to HEK-vector (Table 1). To determine if differences in transport characteristics existed between cell lines, $MMA(GS)_2$ transport by HEK- and HeLa-WT-MRP1-enriched vesicles was compared. Under the conditions tested, $MMA(GS)_2$ (1 μM) transport by HeLa-WT-MRP1 vesicles was 1.6-fold higher ($P < 0.01$) than HEK-WT-MRP1 vesicles (Figure 4A).

Kinetic analysis of MRP1-mediated $MMA(GS)_2$ transport: To determine if the increased transport of $MMA(GS)_2$ was due to changes in K_m and/or V_{max}, MRP1-mediated transport of $MMA(GS)_2$ was measured at an initial rate over eight different concentrations of $MMA(GS)_2$ (Figure 4B and Table 2). HEK- and HeLa-WT-MRP1 membrane vesicles, were found to have similar apparent affinity for $MMA(GS)_2$ (K_m of 23 ± 2.2 μM and 33 ± 24 μM, respectively), similar to what we have previously reported for HEK-WT-MRP1 (Carew et al., 2011). In contrast, the V_{max} was 3.4-fold higher for $MMA(GS)_2$ transport by HeLa-WT-MRP1 (V_{max} of 17 ± 5.3 nmol mg^{-1} min^{-1}) than HEK-WT-MRP1 (V_{max} of 4.9 ± 0.5 nmol mg^{-1}

DMD Fast Forward. Published on May 11, 2018 as DOI: 10.1124/dmd.117.079640
This article has not been copyedited and formatted. The final version may differ from this version.

min^{-1}) membrane vesicles (Figure 4B and Table 2). In addition, kinetic characterization of MMA(GS)$_2$ transport by the double dephosphorylation-mimicking mutant HEK-Y920F/S921A-MRP1, previously demonstrated to have substantially reduced apparent K_m and V_{max} values for As(GS)$_3$ relative to HEK-WT-MRP1(Shukalek et al., 2016) was completed. Interestingly, HEK-Y920F/S921A-MRP1 had very similar apparent affinity (K_m of 24 ± 5.5 μM) and capacity (V_{max} of 5.3 ± 2.2 nmol mg^{-1} min^{-1}) to that of HEK-WT-MRP1 (Figure 4B and Table 2). Consistent with this, the phosphorylation-mimicking mutant HEK-Y920E/S921E-MRP1 also had similar apparent affinity and capacity to HEK-WT-MRP1 (mean K_m of 24 μM, V_{max} of 5.5 nmol mg^{-1} protein min^{-1}, n=2) (Table 2). These data suggest that, in contrast with As(GS)$_3$ transport, phosphorylation of Y920/S921 has little influence on the transport of MMA(GS)$_2$ by MRP1.

Inhibition of As(GS)$_3$ transport by MMA(GS)$_2$: While the K_m of As(GS)$_3$ for MRP1 was >10-fold higher for HEK-WT-MRP1 compared with HeLa-WT-MRP1 and HEK-Y920F/S921A-MRP1 (Shukalek et al., 2016), no difference between the apparent K_m value for MMA(GS)$_2$ transport was observed for these membrane vesicles (Figure 4 and Table 2). This result suggested that MMA(GS)$_2$ and As(GS)$_3$ interact at non-identical binding sites. To begin to characterize the differences in interaction of As(GS)$_3$ and MMA(GS)$_2$ with MRP1, transport of As(GS)$_3$ (1 μM) by HEK-WT-MRP1 vesicles was measured in the presence of increasing concentrations of MMA(GS)$_2$ (Figure 5A). MMA(GS)$_2$ was found to potently inhibit As(GS)$_3$ transport with an IC_{50} value of 11 ± 1.5 μM.

The inhibition of As(GS)$_3$ transport by MMA(GS)$_2$ was further characterized by measuring the effect of MMA(GS)$_2$ (5, 10, and 15 μM) on As(GS)$_3$ (0.1-20 μM) transport (15 μM shown in Figure 5B). Michaelis-Menten analysis showed that MMA(GS)$_2$ at each concentration tested reduced both the apparent K_m and V_{max} values, suggesting an uncompetitive mode of inhibition with an average K_i of 7.3 ± 5.1 μM (± S.D., n=3). These

DMD Fast Forward. Published on May 11, 2018 as DOI: 10.1124/dmd.117.079640
This article has not been copyedited and formatted. The final version may differ from this version.

data are consistent with $MMA(GS)_2$ and $As(GS)_3$ interacting at non-identical binding sites.

DMD Fast Forward. Published on May 11, 2018 as DOI: 10.1124/dmd.117.079640
This article has not been copyedited and formatted. The final version may differ from this version.

Discussion

The proven human carcinogen arsenic naturally contaminates the drinking water of hundreds of millions of people world-wide. One of the most affected countries is Bangladesh, where the arsenic contamination has been referred to as "the largest mass poisoning of a population in history" (Smith et al., 2000). Understanding the cellular handling of arsenic, including efflux pathways, is critical for the prevention and treatment of arsenic-induced disease.

We have investigated the ability of MRP1 to confer resistance to and/or transport important methylated arsenic metabolites when expressed in HEK293 cells compared to HeLa cells. The cellular resistance conferred by MRP1 against different arsenic species is useful information, however, resistance levels can be influenced by cellular metabolism and uptake efficiency. To draw conclusions about MRP1-mediated transport of specific arsenic compounds it was critical to measure their transport directly using MRP1-enriched membrane vesicles. The population of membrane vesicles that are accumulating MRP1 substrates are inside-out, allowing the measurement of ATP-dependent transport with minimal influence of metabolism and cellular uptake. This allows the MRP1 contribution to cellular export of specific arsenic compunds to be evaluated, and allows the accurate determination of kinetic parameters.

The most pronounced difference between cell lines was for DMA^{V}, which HEK-MRP1 cells conferred resistance to and HEK-WT-MRP1 membrane vesicles transported with high apparent affinity and capacity (Table 1 and Figure 2). This is the first report that MRP1 is capable of transporting this important arsenic metabolite. In contrast, HeLa-MRP1 cells did not confer resistance to DMA^{V} relative to HeLa-vector cells (Carew et al., 2011), and HeLa-WT-MRP1 membrane vesicles did not have detectable DMA^{V} transport activity (Figure 2A).

DMD Fast Forward. Published on May 11, 2018 as DOI: 10.1124/dmd.117.079640
This article has not been copyedited and formatted. The final version may differ from this version.

The relative resistance conferred by MRP1 expressed in HEK293 cells was small, but significant (1.4-fold, $P < 0.05$, Figure 1C and Table 1). This marginal resistance was in contrast with the high affinity and high capacity transport of DMA^V observed with HEK-WT-MRP1-enriched membrane vesicles (Figure 2C and Table 2). A likely explanation for the difference in results between the two assays is that DMA^V is poorly taken up by cells (Delnomdedieu et al., 1995; Dopp et al., 2004; Dopp et al., 2005; Naranmandura et al., 2007; Naranmandura et al., 2011), including HEK293 cells (Banerjee et al., 2014). Thus, it is likely that the data generated with the inside-out MRP1-enriched membrane vesicles, with no requirement for cell entry, more accurately reflects what is occurring after formation of DMA^V within the cell. Humans are predominantly exposed to As^{III} and As^V in drinking water, which are taken up by cells efficiently (Roggenbeck et al., 2016), and then converted to methylated products (e.g., DMA^V).

As a starting point for determining a mechanism for cell line differences in MRP1-mediated DMA^V transport, we investigated the potential contribution of differential phosphorylation. Mutation of two phosphorylation sites (Y920/S921-MRP1), previously reported as responsible for cell line differences in the transport of $As(GS)_3$, to both phospho- or dephospho-mimicking amino acids, surprisingly resulted in a complete loss of DMA^V transport. Individual mutant HEK-Y920F-MRP1 and HEK-S921A-MRP1 membrane vesicles, shown previously to transport $As(GS)_3$ to a similar extent as HEK-WT-MRP1, also completely lacked DMA^V transport. The inclusion of a PIC during the preparation of HeLa-WT-MRP1 membrane vesicles did not result in a gain of DMA^V transport activity (although MRP1-mediated $As(GS)_3$ transport was increased), suggesting that either phosphorylation was not important or a stable phosphorylation site (not influenced by the PIC) was involved. Mutation of multiple other putative phosphorylation sites in the linker region also resulted in a complete loss of HEK-MRP1 DMA^V transport. Our data suggest that DMA^V transport by

DMD Fast Forward. Published on May 11, 2018 as DOI: 10.1124/dmd.117.079640
This article has not been copyedited and formatted. The final version may differ from this version.

HEK-WT-MRP1 membrane vesicles is extremely sensitive to alterations in the linker region between NBD1 and MSD2. The reasons for this are currently not understood and require further investigation. Differences in post-translational modifications and/or protein:protein interactions that alter the structure of this region could potentially explain the cell line differences in MRP1-mediated DMA^V transport. Indeed, there is some suggestion in the literature that this linker region is important for protein:protein interactions and that such interactions may be modulated by phosphorylation (Yang et al., 2012; Ambadipudi and Georges, 2017).

MRP1 transport of DMA^V is the second DMA^V efflux pathway to be identified. Previously, we reported that the related MRP4 transports DMA^V with similar affinity ($K_{0.5}$ 0.22 ± 0.15 μM for MRP4 versus K_m 0.19 ± 0.06 μM for MRP1), but through a co-operative mechanism (Hill coefficient 2.9 ± 1.2) and assuming equal protein levels, lower capacity (V_{max} 32 ± 3 pmol mg^{-1} protein min^{-1} for MRP4 versus V_{max} 342 ± 37 pmol mg^{-1} protein min^{-1} for MRP1) [(Banerjee et al., 2014; Banerjee et al., 2016) and Table 2]. The tissue expression and cellular localization of MRP4 likely make it critical for urinary elimination of hepatic metabolites (Banerjee et al., 2014). The localization of MRP1 to the basolateral surface of epithelial cells and expression in specific cell types of most tissues (undetectable protein levels in human hepatocytes), likely makes MRP1 important for cellular/tissue protection rather than playing a role in arsenic elimination.

DMA^V is an arsenic compound with low toxicity relative to trivalent arsenic species (Moe et al., 2016). The efflux of DMA^V from the cell is critical to prevent the reduction of DMA^V to the highly reactive DMA^{III} (Nemeti and Gregus, 2013). Furthermore, export of DMA^V would likely prevent product inhibition of arsenic (+3 oxidation state) methyltransferase, allowing the formation and cellular export of more DMA^V. The reducing intracellular environment might suggest that DMA^{III} is the predominant form of dimethylated arsenic within the cell, however, this has been difficult to prove and DMA^{V} has been detected in human cell lines and mouse liver homogenate (Currier et al., 2011). The highly reactive DMA^{III} is highly protein bound and unlikely to be available for cellular export (Hippler et al., 2011; Shen et al., 2013). An equilibrium between DMA^{III} and DMA^{V} will exist within the cell, and the high affinity high capacity export of DMA^{V} by MRP1 would provide a good mechanism for cellular detoxification.

Out of the five arsenic compounds tested HEK-MRP1 conferred the highest level of resistance against As^{V} (9-fold) followed by As^{III} (5-fold). Consistent with previous studies using MRP1-enriched membrane vesicles isolated from H69AR cells (Leslie et al., 2004), HEK- and HeLa MRP1-enriched vesicles did not transport As^{V} in the presence or absence of GSH. Once inside the cell As^{V} is reduced to As^{III} and then enters the methylation pathway (Cullen, 2014). Thus, our results are consistent with As^{V} and As^{III} being converted to $As(GS)_3$ prior to efflux by MRP1, as we have shown previously (Leslie et al., 2004). The reason why HEK-MRP1 cells confer higher levels of resistance to As^{V} than As^{III} is not understood. As^{V} enters cells more slowly (through Na^{+}-dependent phosphate transporters) than As^{III} (through aquaglyceroporins) (Mukhopadhyay et al., 2014; Roggenbeck et al., 2016), and this could influence the methylation and glutathionylation of arsenic and alter the metabolites available for MRP1 export.

HEK-MRP1 and HeLa-MRP1 cell lines both conferred significantly higher levels of resistance to MMA^{III} than their respective vector controls [(Carew et al., 2011) and Table 1]. $MMA(GS)_2$ was transported with comparable apparent affinity by HeLa-WT-MRP1 and HEK-WT-MRP1 membrane vesicles, however, the V_{max} was 3.4-fold higher for HeLa-MRP1 membrane vesicles. Kinetic parameters for $MMA(GS)_2$ transport were not significantly different between HEK-WT-MRP1 and HEK-Y920F/S921A-MRP1 or HEK-Y920E/S921E-MRP1, suggesting that differential phosphorylation at these sites is not responsible for the

DMD Fast Forward. Published on May 11, 2018 as DOI: 10.1124/dmd.117.079640
This article has not been copyedited and formatted. The final version may differ from this version.

cell line differences in V_{max}. Consistent with these phosphorylation sites being important for the interaction between MRP1 and $As(GS)_3$, but not MRP1 and $MMA(GS)_2$, we found that $MMA(GS)_2$ was an uncompetitive inhibitor of $As(GS)_3$ transport. Thus, increasing concentrations of $As(GS)_3$ did not overcome $MMA(GS)_2$ inhibition (Figure 5B) providing support for the idea that $As(GS)_3$ and $MMA(GS)_2$ do not share identical binding sites.

Arsenic has previously been reported to activate kinase and inhibit phosphatase pathways (Rehman et al., 2012; Beauchamp et al., 2015), and we had postulated cellular exposure to arsenic would result in a shift to a pro-phosphorylation state of Y920/S921-MRP1 (Shukalek et al., 2016). This in turn would result in the switch of MRP1 from a high-affinity, low capacity transporter of $As(GS)_3$ to a more efficient low affinity, high capacity $As(GS)_3$ transporter (Shukalek et al., 2016). Phosphorylation of these residues appear to be important specifically for $As(GS)_3$, but not for $MMA(GS)_2$ or DMA^V (this study) or as previously reported for methotrexate, LTC_4 or $E_2 17\beta G$ (Loe et al., 1996b; Stride et al., 1997; Shukalek et al., 2016). Why phosphorylation of MRP1 at Y920/S921 has an impact on $As(GS)_3$, but not other arsenic metabolites is unknown. Potentially, MRP1 exports $As(GS)_3$ over a broad concentration range to reduce As^{III} availability for the formation of more toxic trivalent methylated forms. The K_m values for $As(GS)_3$ (K_m range ~0.3-4 μM) (Leslie et al., 2004; Shukalek et al., 2016) and DMA^V (K_m 0.19 μM) (Table 2) are much lower than $MMA(GS)_2$ (K_m range 11-33 μM) [Table 2 and (Carew et al., 2011)]. At low levels of arsenic exposure, MRP1 is potentially important for the export of $As(GS)_3$ and any DMA^V that is formed (preventing the formation of the highly toxic DMA^{III}). During higher cellular arsenic exposure MRP1 phosphorylation allows it to still export $As(GS)_3$ efficiently, $MMA(GS)_2$ accumulation might start to occur and MRP1 would be able to export this as well as DMA^V. It's worth noting that the transport of DMA^V by MRP1 is remarkably more efficient than reported for any other transporter and arsenical combination (Roggenbeck et al., 2016), providing support for MRP1 being an important transport pathway for DMA^V under environmentally relevant exposure conditions.

Differences in MRP1 transport of DMA^V (this study) and $As(GS)_3$ (Shukalek et al., 2016) by membrane vesicles isolated from different cells raises the possibility that MRP1 could have a distinct role in arsenic efflux, depending upon the tissue and/or cell type expressed in. MRP1 has been indirectly implicated in the protection of specific tissues from arsenic toxicity including kidney and brain (Kimura et al., 2005; Kimura et al., 2006; Dringen et al., 2016; Wang et al., 2016). Furthermore, MRP1 could play a role in resistance to arsenic-based therapies and this could be modified depending upon the tumor type. This study lays the groundwork for further investigation into how the cellular environment influences the function of MRP1, particularly for the cellular detoxification of important arsenic metabolites.

Acknowledgements

Diane Swanlund is thanked for outstanding technical assistance. Xiufen Lu is gratefully acknowledged for her assistance with ICP-MS. Dr. Susan P.C. Cole (Queen's University) is thanked for providing the HEK/HeLa-MRP1 and HeLa-vector stable cell lines and the pcDNA3.1(-)MRP1.

The 73-arsenic used in this research was supplied by the United States Department of Energy Office of Science by the Isotope Program in the Office of Nuclear Physics.

Authorship Contributions

Participated in research design: Banerjee, Kaur, Whitlock, Carew, Le, Leslie

Conducted experiments: Banerjee, Kaur, Whitlock, Carew

Contributed new reagents or analytic tools: Le

DMD Fast Forward. Published on May 11, 2018 as DOI: 10.1124/dmd.117.079640
This article has not been copyedited and formatted. The final version may differ from this version.

Performed data analysis: Banerjee, Kaur, Whitlock, Carew, and Leslie

Wrote or contributed to the writing of the manuscript: Banerjee, Kaur, Whitlock, and Leslie

References

Ally MS, Ransohoff K, Sarin K, Atwood SX, Rezaee M, Bailey-Healy I, Kim J, Beachy PA, Chang AL, Oro A, Tang JY and Colevas AD (2016) Effects of Combined Treatment With Arsenic Trioxide and Itraconazole in Patients With Refractory Metastatic Basal Cell Carcinoma. *JAMA Dermatol* **152:**452-456.

Ambadipudi R and Georges E (2017) Sequences in Linker-1 domain of the multidrug resistance associated protein (MRP1 or ABCC1) bind to tubulin and their binding is modulated by phosphorylation. *Biochem Biophys Res Commun* **482:**1001-1006.

Banerjee M, Carew MW, Roggenbeck BA, Whitlock BD, Naranmandura H, Le XC and Leslie EM (2014) A Novel Pathway for Arsenic Elimination: Human Multidrug Resistance Protein 4 (MRP4/ABCC4) Mediates Cellular Export of Dimethylarsinic Acid (DMAV) and the Diglutathione Conjugate of Monomethylarsonous Acid (MMAIII). *Mol Pharmacol* **86:**168-179.

Banerjee M, Marensi V, Conseil G, Le XC, Cole SP and Leslie EM (2016) Polymorphic variants of MRP4/ABCC4 differentially modulate the transport of methylated arsenic metabolites and physiological organic anions. *Biochem Pharmacol* **120:**72-82.

Beauchamp EM, Kosciuczuk EM, Serrano R, Nanavati D, Swindell EP, Viollet B, O'Halloran TV, Altman JK and Platanias LC (2015) Direct binding of arsenic trioxide to AMPK and generation of inhibitory effects on acute myeloid leukemia precursors. *Mol Cancer Ther* **14:**202-212.

Bu N, Wang HY, Hao WH, Liu X, Xu S, Wu B, Anan Y, Ogra Y, Lou YJ and Naranmandura H (2011) Generation of thioarsenicals is dependent on the enterohepatic circulation in rats. *Metallomics* **3:**1064-1073.

Carew MW and Leslie EM (2010) Selenium-dependent and -independent transport of arsenic by the human multidrug resistance protein 2 (MRP2/ABCC2): implications for the

DMD Fast Forward. Published on May 11, 2018 as DOI: 10.1124/dmd.117.079640
This article has not been copyedited and formatted. The final version may differ from this version.

mutual detoxification of arsenic and selenium. *Carcinogenesis* **31:**1450-1455.

Carew MW, Naranmandura H, Shukalek CB, Le XC and Leslie EM (2011) Monomethylarsenic diglutathione transport by the human multidrug resistance protein 1 (MRP1/ABCC1). *Drug Metab Dispos* **39:**2298-2304.

Cicconi L and Lo-Coco F (2016) Current management of newly diagnosed acute promyelocytic leukemia. *Annals of Oncology* **27:**1474-1481.

Cole SP (2014) Multidrug resistance protein 1 (MRP1, ABCC1), a "multitasking" ATP-binding cassette (ABC) transporter. *J Biol Chem* **289:**30880-30888.

Cole SP and Deeley RG (2006) Transport of glutathione and glutathione conjugates by MRP1. *Trends Pharmacol Sci* **27:**438-446.

Conseil G and Cole SP (2013) Two polymorphic variants of ABCC1 selectively alter drug resistance and inhibitor sensitivity of the multidrug and organic anion transporter multidrug resistance protein 1. *Drug Metab Dispos* **41:**2187-2196.

Cui X, Kobayashi Y, Hayakawa T and Hirano S (2004) Arsenic speciation in bile and urine following oral and intravenous exposure to inorganic and organic arsenics in rats. *Toxicol Sci* **82:**478-487.

Cullen WR (2014) Chemical mechanism of arsenic biomethylation. *Chem Res Toxicol* **27:**457-461.

Cullen WR, Liu Q, Lu X, McKnight-Whitford A, Peng H, Popowich A, Yan X, Zhang Q, Fricke M, Sun H and Le XC (2016) Methylated and thiolated arsenic species for environmental and health research - A review on synthesis and characterization. *J Environ Sci (China)* **49:**7-27.

Currier JM, Svoboda M, de Moraes DP, Matousek T, Dedina J and Styblo M (2011) Direct analysis of methylated trivalent arsenicals in mouse liver by hydride generation-cryotrapping-atomic absorption spectrometry. *Chem Res Toxicol* **24:**478-480.

DMD Fast Forward. Published on May 11, 2018 as DOI: 10.1124/dmd.117.079640
This article has not been copyedited and formatted. The final version may differ from this version.

Delnomdedieu M, Styblo M and Thomas DJ (1995) Time dependence of accumulation and binding of inorganic and organic arsenic species in rabbit erythrocytes. *Chem Biol Interact* **98:**69-83.

Dopp E, Hartmann LM, Florea AM, von Recklinghausen U, Pieper R, Shokouhi B, Rettenmeier AW, Hirner AV and Obe G (2004) Uptake of inorganic and organic derivatives of arsenic associated with induced cytotoxic and genotoxic effects in Chinese hamster ovary (CHO) cells. *Toxicol Appl Pharmacol* **201:**156-165.

Dopp E, Hartmann LM, von Recklinghausen U, Florea AM, Rabieh S, Zimmermann U, Shokouhi B, Yadav S, Hirner AV and Rettenmeier AW (2005) Forced uptake of trivalent and pentavalent methylated and inorganic arsenic and its cyto-/genotoxicity in fibroblasts and hepatoma cells. *Toxicol Sci* **87:**46-56.

Dringen R, Spiller S, Neumann S and Koehler Y (2016) Uptake, Metabolic Effects and Toxicity of Arsenate and Arsenite in Astrocytes. *Neurochem Res* **41:**465-475.

Drobna Z, Naranmandura H, Kubachka KM, Edwards BC, Herbin-Davis K, Styblo M, Le XC, Creed JT, Maeda N, Hughes MF and Thomas DJ (2009) Disruption of the arsenic (+3 oxidation state) methyltransferase gene in the mouse alters the phenotype for methylation of arsenic and affects distribution and retention of orally administered arsenate. *Chem Res Toxicol* **22:**1713-1720.

Drobna Z, Walton FS, Harmon AW, Thomas DJ and Styblo M (2010) Interspecies differences in metabolism of arsenic by cultured primary hepatocytes. *Toxicol Appl Pharmacol* **245:**47-56.

Falchi L, Verstovsek S, Ravandi-Kashani F and Kantarjian HM (2016) The evolution of arsenic in the treatment of acute promyelocytic leukemia and other myeloid neoplasms: Moving toward an effective oral, outpatient therapy. *Cancer* **122:**1160-1168.

DMD Fast Forward. Published on May 11, 2018 as DOI: 10.1124/dmd.117.079640
This article has not been copyedited and formatted. The final version may differ from this version.

Hipfner DR, Gauldie SD, Deeley RG and Cole SP (1994) Detection of the M(r) 190,000 multidrug resistance protein, MRP, with monoclonal antibodies. *Cancer Res* **54:**5788-5792.

Hippler J, Zdrenka R, Reichel RAD, Weber DG, Rozynek P, Johnen G, Dopp E and Hirnera AV (2011) Intracellular, time-resolved speciation and quantification of arsenic compounds in human urothelial and hepatoma cells. *J Anal At Spectrom* **26:**2396-2403.

Hughes MF, Edwards BC, Herbin-Davis KM, Saunders J, Styblo M and Thomas DJ (2010) Arsenic (+3 oxidation state) methyltransferase genotype affects steady-state distribution and clearance of arsenic in arsenate-treated mice. *Toxicol Appl Pharmacol* **249:**217-223.

IARC (2012) Arsenic, metals, fibres, and dusts. *IARC Monogr Eval Carcinog Risks Hum* **100:**11-465.

Ito K, Olsen SL, Qiu W, Deeley RG and Cole SP (2001) Mutation of a single conserved tryptophan in multidrug resistance protein 1 (MRP1/ABCC1) results in loss of drug resistance and selective loss of organic anion transport. *J Biol Chem* **276:**15616-15624.

Jedlitschky G, Leier I, Buchholz U, Barnouin K, Kurz G and Keppler D (1996) Transport of glutathione, glucuronate, and sulfate conjugates by the MRP gene-encoded conjugate export pump. *Cancer Res* **56:**988-994.

Kala SV, Kala G, Prater CI, Sartorelli AC and Lieberman MW (2004) Formation and urinary excretion of arsenic triglutathione and methylarsenic diglutathione. *Chem Res Toxicol* **17:**243-249.

Kala SV, Neely MW, Kala G, Prater CI, Atwood DW, Rice JS and Lieberman MW (2000) The MRP2/cMOAT transporter and arsenic-glutathione complex formation are required for biliary excretion of arsenic. *J Biol Chem* **275:**33404-33408.

Khairul I, Wang QQ, Jiang YH, Wang C and Naranmandura H (2017) Metabolism, toxicity and anticancer activities of arsenic compounds. *Oncotarget* **8:**23905-23926.

Kimura A, Ishida Y, Hayashi T, Wada T, Yokoyama H, Sugaya T, Mukaida N and Kondo T (2006) Interferon-gamma plays protective roles in sodium arsenite-induced renal injury by up-regulating intrarenal multidrug resistance-associated protein 1 expression. *Am J Pathol* **169:**1118-1128.

Kimura A, Ishida Y, Wada T, Yokoyama H, Mukaida N and Kondo T (2005) MRP-1 expression levels determine strain-specific susceptibility to sodium arsenic-induced renal injury between C57BL/6 and BALB/c mice. *Toxicol Appl Pharmacol* **203:**53-61.

Kligerman AD, Doerr CL, Tennant AH, Harrington-Brock K, Allen JW, Winkfield E, Poorman-Allen P, Kundu B, Funasaka K, Roop BC, Mass MJ and DeMarini DM (2003) Methylated trivalent arsenicals as candidate ultimate genotoxic forms of arsenic: Induction of chromosomal mutations but not gene mutations. *Environ Mol Mutagen* **42:**192-205.

Kritharis A, Bradley TP and Budman DR (2013) The evolving use of arsenic in pharmacotherapy of malignant disease. *Ann Hematol* **92:**719-730.

Leslie EM (2012) Arsenic-glutathione conjugate transport by the human multidrug resistance proteins (MRPs/ABCCs). *J Inorg Biochem* **108:**141-149.

Leslie EM, Bowers RJ, Deeley RG and Cole SP (2003) Structural requirements for functional interaction of glutathione tripeptide analogs with the human multidrug resistance protein 1 (MRP1). *J Pharmacol Exp Ther* **304:**643-653.

Leslie EM, Deeley RG and Cole SP (2005) Multidrug resistance proteins: role of P-glycoprotein, MRP1, MRP2, and BCRP (ABCG2) in tissue defense. *Toxicol Appl*

Pharmacol **204:**216-237.

Leslie EM, Haimeur A and Waalkes MP (2004) Arsenic transport by the human multidrug resistance protein 1 (MRP1/ABCC1). Evidence that a tri-glutathione conjugate is required. *J Biol Chem* **279:**32700-32708.

Loe DW, Almquist KC, Cole SP and Deeley RG (1996a) ATP-dependent 17 beta-estradiol 17-(beta-D-glucuronide) transport by multidrug resistance protein (MRP). Inhibition by cholestatic steroids. *J Biol Chem* **271:**9683-9689.

Loe DW, Almquist KC, Deeley RG and Cole SP (1996b) Multidrug resistance protein (MRP)-mediated transport of leukotriene C4 and chemotherapeutic agents in membrane vesicles. Demonstration of glutathione-dependent vincristine transport. *J Biol Chem* **271:**9675-9682.

Mass MJ, Tennant A, Roop BC, Cullen WR, Styblo M, Thomas DJ and Kligerman AD (2001) Methylated trivalent arsenic species are genotoxic. *Chem Res Toxicol* **14:**355-361.

Moe B, Peng H, Lu X, Chen B, Chen LW, Gabos S, Li XF and Le XC (2016) Comparative cytotoxicity of fourteen trivalent and pentavalent arsenic species determined using real-time cell sensing. *J Environ Sci (China)* **49:**113-124.

Mukhopadhyay R, Bhattacharjee H and Rosen BP (2014) Aquaglyceroporins: generalized metalloid channels. *Biochim Biophys Acta* **1840:**1583-1591.

Naranmandura H, Carew MW, Xu S, Lee J, Leslie EM, Weinfeld M and Le XC (2011) Comparative toxicity of arsenic metabolites in human bladder cancer EJ-1 cells. *Chem Res Toxicol* **24:**1586-1596.

Naranmandura H, Ibata K and Suzuki KT (2007) Toxicity of dimethylmonothioarsinic acid toward human epidermoid carcinoma A431 cells. *Chem Res Toxicol* **20:**1120-1125.

Naujokas MF, Anderson B, Ahsan H, Aposhian HV, Graziano JH, Thompson C and Suk WA

(2013) The broad scope of health effects from chronic arsenic exposure: update on a worldwide public health problem. *Environ Health Perspect* **121:**295-302.

Nemeti B and Gregus Z (2013) Reduction of dimethylarsinic acid to the highly toxic dimethylarsinous acid by rats and rat liver cytosol. *Chem Res Toxicol* **26:**432-443.

Petrick JS, Ayala-Fierro F, Cullen WR, Carter DE and Vasken Aposhian H (2000) Monomethylarsonous acid (MMA(III)) is more toxic than arsenite in Chang human hepatocytes. *Toxicol Appl Pharmacol* **163:**203-207.

Platanias LC (2009) Biological responses to arsenic compounds. *J Biol Chem* **284:**18583-18587.

Rahman MM, Ng JC and Naidu R (2009) Chronic exposure of arsenic via drinking water and its adverse health impacts on humans. *Environ Geochem Health* **31 Suppl 1:**189-200.

Reay PF and Asher CJ (1977) Preparation and purification of 74As-labeled arsenate and arsenite for use in biological experiments. *Anal Biochem* **78:**557-560.

Rehman K, Chen Z, Wang WW, Wang YW, Sakamoto A, Zhang YF, Naranmandura H and Suzuki N (2012) Mechanisms underlying the inhibitory effects of arsenic compounds on protein tyrosine phosphatase (PTP). *Toxicol Appl Pharmacol* **263:**273-280.

Roggenbeck BA, Banerjee M and Leslie EM (2016) Cellular arsenic transport pathways in mammals. *J Environ Sci (China)* **49:**38-58.

Shen S, Li XF, Cullen WR, Weinfeld M and Le XC (2013) Arsenic binding to proteins. *Chem Rev* **113:**7769-7792.

Shukalek CB, Swanlund DP, Rousseau RK, Weigl KE, Marensi V, Cole SP and Leslie EM (2016) Arsenic Triglutathione [As(GS)3] Transport by Multidrug Resistance Protein 1 (MRP1/ABCC1) is Selectively Modified by Phosphorylation of Tyr920/Ser921 and Glycosylation of Asn19/Asn23. *Mol Pharmacol* **90:**127-139.

Smith AH, Lingas EO and Rahman M (2000) Contamination of drinking-water by arsenic in

Bangladesh: a public health emergency. *Bull World Health Organ* **78:**1093-1103.

Stride BD, Grant CE, Loe DW, Hipfner DR, Cole SPC and Deeley RG (1997) Pharmacological characterization of the murine and human orthologs of multidrug resistance protein in transfected human embryonic kidney cells. *Mol Pharmacol* **52:**344-353.

Styblo M, Del Razo LM, Vega L, Germolec DR, LeCluyse EL, Hamilton GA, Reed W, Wang C, Cullen WR and Thomas DJ (2000) Comparative toxicity of trivalent and pentavalent inorganic and methylated arsenicals in rat and human cells. *Arch Toxicol* **74:**289-299.

Suzuki KT, Tomita T, Ogra Y and Ohmichi M (2001) Glutathione-conjugated arsenics in the potential hepato-enteric circulation in rats. *Chem Res Toxicol* **14:**1604-1611.

Thomas DJ, Li J, Waters SB, Xing W, Adair BM, Drobna Z, Devesa V and Styblo M (2007) Arsenic (+3 oxidation state) methyltransferase and the methylation of arsenicals. *Exp Biol Med (Maywood)* **232:**3-13.

Thomas DJ, Waters SB and Styblo M (2004) Elucidating the pathway for arsenic methylation. *Toxicol Appl Pharmacol* **198:**319-326.

Vahter M (1999) Methylation of inorganic arsenic in different mammalian species and population groups. *Sci Prog* **82 (Pt 1):**69-88.

Wang QQ, Thomas DJ and Naranmandura H (2015) Importance of being thiomethylated: formation, fate, and effects of methylated thioarsenicals. *Chem Res Toxicol* **28:**281-289.

Wang Y, Chen M, Zhang Y, Huo T, Fang Y, Jiao X, Yuan M and Jiang H (2016) Effects of realgar on GSH synthesis in the mouse hippocampus: Involvement of system XAG(-), system XC(-), MRP-1 and Nrf2. *Toxicol Appl Pharmacol* **308:**91-101.

Yang Y, Li Z, Mo W, Ambadipudi R, Arnold RJ, Hrncirova P, Novotny MV, Georges E and

DMD Fast Forward. Published on May 11, 2018 as DOI: 10.1124/dmd.117.079640
This article has not been copyedited and formatted. The final version may differ from this version.

Zhang JT (2012) Human ABCC1 interacts and colocalizes with ATP synthase alpha, revealed by interactive proteomics analysis. *J Proteome Res* **11:**1364-1372.

Yokohira M, Arnold LL, Pennington KL, Suzuki S, Kakiuchi-Kiyota S, Herbin-Davis K, Thomas DJ and Cohen SM (2010) Severe systemic toxicity and urinary bladder cytotoxicity and regenerative hyperplasia induced by arsenite in arsenic (+3 oxidation state) methyltransferase knockout mice. A preliminary report. *Toxicol Appl Pharmacol* **246:**1-7.

Yokohira M, Arnold LL, Pennington KL, Suzuki S, Kakiuchi-Kiyota S, Herbin-Davis K, Thomas DJ and Cohen SM (2011) Effect of sodium arsenite dose administered in the drinking water on the urinary bladder epithelium of female arsenic (+3 oxidation state) methyltransferase knockout mice. *Toxicol Sci* **121:**257-266.

DMD Fast Forward. Published on May 11, 2018 as DOI: 10.1124/dmd.117.079640
This article has not been copyedited and formatted. The final version may differ from this version.

Footnotes

This work was supported by the Canadian Institutes of Health Research [CIHR grant MOP-272075]. MB was supported by an Alberta Cancer Foundation Cancer Research Postdoctoral Fellowship award, XCL holds the Canada Research Chair in Bioanalytical Technology and Environmental Health. GK holds a Queen Elizabeth II doctoral scholarship and a Medical Sciences Graduate Program Scholarship from the University of Alberta. EML was an Alberta Innovates Health Solutions Scholar and a CIHR New Investigator.

Address correspondence to: Dr. Elaine M. Leslie, 7-08A Medical Sciences Building, Department of Physiology, University of Alberta, Edmonton, AB, Canada, T6G 2H7; Email: eleslie@ualberta.ca; Tel: (780) 492-9250.

DMD Fast Forward. Published on May 11, 2018 as DOI: 10.1124/dmd.117.079640
This article has not been copyedited and formatted. The final version may differ from this version.

Figure legends

Figure 1: Effect of selected arsenic compounds on the viability of HEK293 cells stably expressing human MRP1. Cells expressing empty vector (HEK-vector) (○) and MRP1 (HEK-MRP1) (●) were incubated in the presence of (A) As^{III}, (B) As^{V}, (C) MMA^{III}, or (D) DMA^{V} for 72 h. Cell viability was determined using a tetrazolium-based cytotoxicity assay. Data points are means (± S.D.) of quadruplicate determinations in a representative experiment; similar results were obtained in at least two additional experiments (mean relative resistance data from independent experiments are shown in Table 1).

Figure 2: ATP-dependent transport of DMA^{V} by MRP1-enriched membrane vesicles. Transport experiments were done with membrane vesicles (20 µg of protein) prepared from HEK293T cells transiently transfected with WT-MRP1 (black bars or symbols) or empty pcDNA3.1(-) (vector) (white bars or symbols) or HeLa cells stably transfected with WT-MRP1 (dark gray bars) or empty vector (light gray bars). For individual experiments, transport was done in triplicate, and then reactions were pooled for analysis by ICP-MS. Bars and symbols represent the means (± S.D.) of three independent experiments. (A) Vesicles were incubated for 20 sec at 37°C in transport buffer with DMA^{V} (0.05 or 1 µM). Statistically significant differences in DMA^{V} transport were determined using a one way ANOVA followed by a Dunnett's multiple comparisons post hoc test with HEK-Vector as the control group (***$p < 0.001$; ****$p < 0.0001$). (B) Time course of ATP-dependent DMA^{V} transport was determined by incubating membrane vesicles with DMA^{V} (1 µM) in transport buffer at 37°C for the indicated time points. (C) HEK-WT-MRP1 membrane vesicles were incubated for 20 sec at 37°C with increasing concentrations of DMA^{V} (0.025–2.5 µM). Data were fitted using a one-site Michaelis-Menten kinetic model with GraphPad Prism®6.

DMD Fast Forward. Published on May 11, 2018 as DOI: 10.1124/dmd.117.079640
This article has not been copyedited and formatted. The final version may differ from this version.

Figure 3: Effect of Y920/S921-MRP1 mutation and/or phosphatase inhibitors on ATP-dependent transport of DMA^V or $As(GS)_3$ by MRP1-enriched membrane vesicles. Transport experiments were done with membrane vesicles (20 µg of protein) prepared from HEK293T cells transiently transfected with WT-MRP1, Y920F/S921A-MRP1, Y920E/S921E-MRP1, or empty pcDNA3.1 (-) (vector) or from HeLa cells stably transfected with WT-MRP1 or empty vector. Bars and symbols represent the means (± S.D.) of three independent experiments. (A) Membrane vesicles from HEK293T cells transiently transfected with WT-MRP1 (dark gray bars), Y920F/S921A-MRP1 (light gray bars), Y920E/S921E-MRP1 (black bars), or vector (white bars) were incubated for 20 sec at 37°C with DMA^V (1 µM). For individual experiments, transport was done in triplicate, and then reactions were pooled for analysis by ICP-MS. Statistically significant differences in DMA^V transport were determined using a one way ANOVA followed by a Dunnett's multiple comparisons post hoc test using HEK-Vector as the control group (****$p < 0.0001$). (B) Membrane vesicles from HeLa cells stably transfected with vector (light gray bars), or WT-MRP1 prepared in the presence (white bars) or absence (black bars) of a PIC were incubated for 20 sec at 37°C with DMA^V (0.05 or 1 µM). HEK-WT-MRP1 membrane vesicles were used as a positive control. For individual experiments, transport was done in triplicate, and then reactions were pooled for analysis by ICP-MS. Statistically significant differences in DMA^V transport were determined using a one way ANOVA followed by a Dunnett's multiple comparisons post hoc test using HeLa-Vector as the control group (*$p < 0.05$; ****$p < 0.0001$). (C) ATP-dependent transport of $As(GS)_3$ by MRP1-enriched membrane vesicles from stably transfected HeLa cells prepared with (white bar) or without (black bar) PIC. The membrane vesicles were incubated for 3 min at 37°C with $As(GS)_3$ (1 µM). Statistically significant differences in $As(GS)_3$ transport were determined using an unpaired two-tailed t-test (**$p < 0.01$).

DMD Fast Forward. Published on May 11, 2018 as DOI: 10.1124/dmd.117.079640
This article has not been copyedited and formatted. The final version may differ from this version.

Figure 4: ATP-dependent transport of $MMA(GS)_2$ by MRP1-enriched membrane vesicles. Transport experiments were done with membrane vesicles (20 µg of protein) prepared from HEK293T cells transiently transfected with WT-MRP1, Y920F/S921A-MRP1, or empty pcDNA3.1(-) (vector) or from HeLa cells stably transfected with WT-MRP1 or vector. For individual experiments, transport was done in triplicate, and then reactions were pooled for analysis by ICP-MS. Bars and symbols represent the means (+ S.D.) of at least three independent experiments. (A) Vesicles prepared from HEK293T cells transiently transfected with WT-MRP1 (dark gray bars) or vector (white bars) or HeLa cells stably transfected with WT-MRP1 (black bars) or vector (light gray bars) were incubated for 1 min at 37°C in transport buffer with $MMA(GS)_2$ (1 µM). Statistically significant differences in $MMA(GS)_2$ transport were determined using a one way ANOVA followed by a Dunnett's multiple comparisons post hoc test using HEK-WT-MRP1 as the control group (**$p < 0.01$; ****$p < 0.0001$). (B) Vesicles prepared from HEK293T cells transiently transfected with WT-MRP1 or Y920F/S921A-MRP1or from HeLa cells stably transfected with WT-MRP1 were incubated for 1 min at 37°C with increasing concentrations of $MMA(GS)_2$ (1–200 µM). Data were fitted using a one-site Michaelis-Menten kinetic model with GraphPad Prism®6.

Figure 5: $MMA(GS)_2$ inhibits MRP1 mediated ATP-dependent transport of $As(GS)_3$. Transport experiments were done with membrane vesicles (20 µg of protein) prepared from HEK293T cells transiently transfected with WT-MRP1. Individual experiments were done in triplicate and ^{73}As quantified using liquid scintillation counting. (A) Vesicles were incubated with $^{73}As(GS)_3$ (1 µM, 40 nCi) for 3 min at 37°C in transport buffer with increasing concentrations of $MMA(GS)_2$ (0.01–300 µM). Symbol represents the mean (+ S.D.) of three independent experiments. (B) Vesicles were incubated with increasing concentrations of

DMD Fast Forward. Published on May 11, 2018 as DOI: 10.1124/dmd.117.079640
This article has not been copyedited and formatted. The final version may differ from this version.

$^{73}As(GS)_3$ (0.1–20 μM, 40-100 nCi) for 3 min at 37°C in transport buffer in presence of $MMA(GS)_2$ (15 μM). Data points represent means (+ S.D.) of triplicate determinations in a single experiment. Two independent additional experiments with $MMA(GS)_2$ at 5 and 10 μM were done in order to calculate the K_i (7.3 ± 5.1 μM, ± S.D., n=3).

DMD Fast Forward. Published on May 11, 2018 as DOI: 10.1124/dmd.117.079640

Table 1

Resistance of MRP1-transfected HEK293 and HeLa cells to inorganic and methylated arsenic species.

	IC_{50} (± S.D.)			IC_{50} (± S.D.)		
	HEK-vector	HEK-MRP1	Relative Resistance	HeLa-vector	HeLa-MRP1	Relative Resistance
As^{III}	4.9 ± 1.0	25.5 ± 4.2	**5.3 ± 0.9********	7.0 ± 1.2	17.5 ± 2.4	**2.5±0.3*******
As^{V}	26 ± 6.7	221 ± 62	**9.2 ± 3.6*******	156±55	303±51	**2.1 ± 0.5******
MMA^{III}	1.7 ± 0.12	3.9 ± 0.5	**2.3 ± 0.2*******	5.0 ± 1.2	7.6 ± 1.3	**1.5 ± 0.2***
DMA^{III}	1.2 ± 1	1.6 ± 1.6	**1.2 ± 0.2**	6 ± 0.5[b]	7 ± 2.3 [b]	**1.2 ± 0.4** [b]
DMA^{V}	1090 ± 290	1500 ± 250	**1.4 ± 0.2***	690 ± 430	680 ± 450	**1.0 ± 0.13**

[a] The resistance of HEK293 and HeLa cell lines expressing wild-type MRP1 was determined using an MTS assay and relative resistance factors calculated by dividing the IC_{50} values obtained for the MRP1-expressing cell line by the IC_{50} values obtained for empty vector expressing cell line. Values shown are the mean (± S.D.) obtained from at least three independent experiments.

[b]Previously published in (Carew et al., 2011) but done in parallel experiments with unpublished HEK data.

The IC_{50} values for the MRP1 expressing cell lines were compared with the IC_{50} values for the empty vector control cell lines using a Student's t-test (* P < 0.05, ** P < 0.01, *** P < 0.001, **** P < 0.0001).

DMD Fast Forward. Published on May 11, 2018 as DOI: 10.1124/dmd.117.079640
This article has not been copyedited and formatted. The final version may differ from this version.

Table 2

Kinetic parameters of $MMA(GS)_2$ and DMA^V transport by MRP1 (and phosphorylation mutants)

				Kinetic parameter	
Compound	**Cell Line**	**Variant**	***n***	***K_m*** (μM)	***V_{max}***[a]
DMA^V	HEK293T	WT	3	0.19 ± 0.06	342 ± 37[b]
$MMA(GS)_2$	HEK293T	WT	3	23 ± 2.2	4.9 ± 0.5
		Y920F/S921A	4	24 ± 5.5	5.3 ± 2.2
		Y920E/S921E	2	29, 18	5.8, 5.0
	HeLa	WT	3	33 ± 24	16.8 ± 5.3**

[a]V_{max} values are in nmol mg^{-1} protein min^{-1} unless otherwise indicated and were corrected for MRP1-level relative to HEK-WT-MRP1 as described in Materials and Methods.

[b]pmol mg^{-1} protein min^{-1}

**significantly different from HEK293-MRP1 (P<0.01 One way ANOVA with Tukey's multiple comparisons post-hoc test).

FIGURE 1 (Banerjee *et al.*)

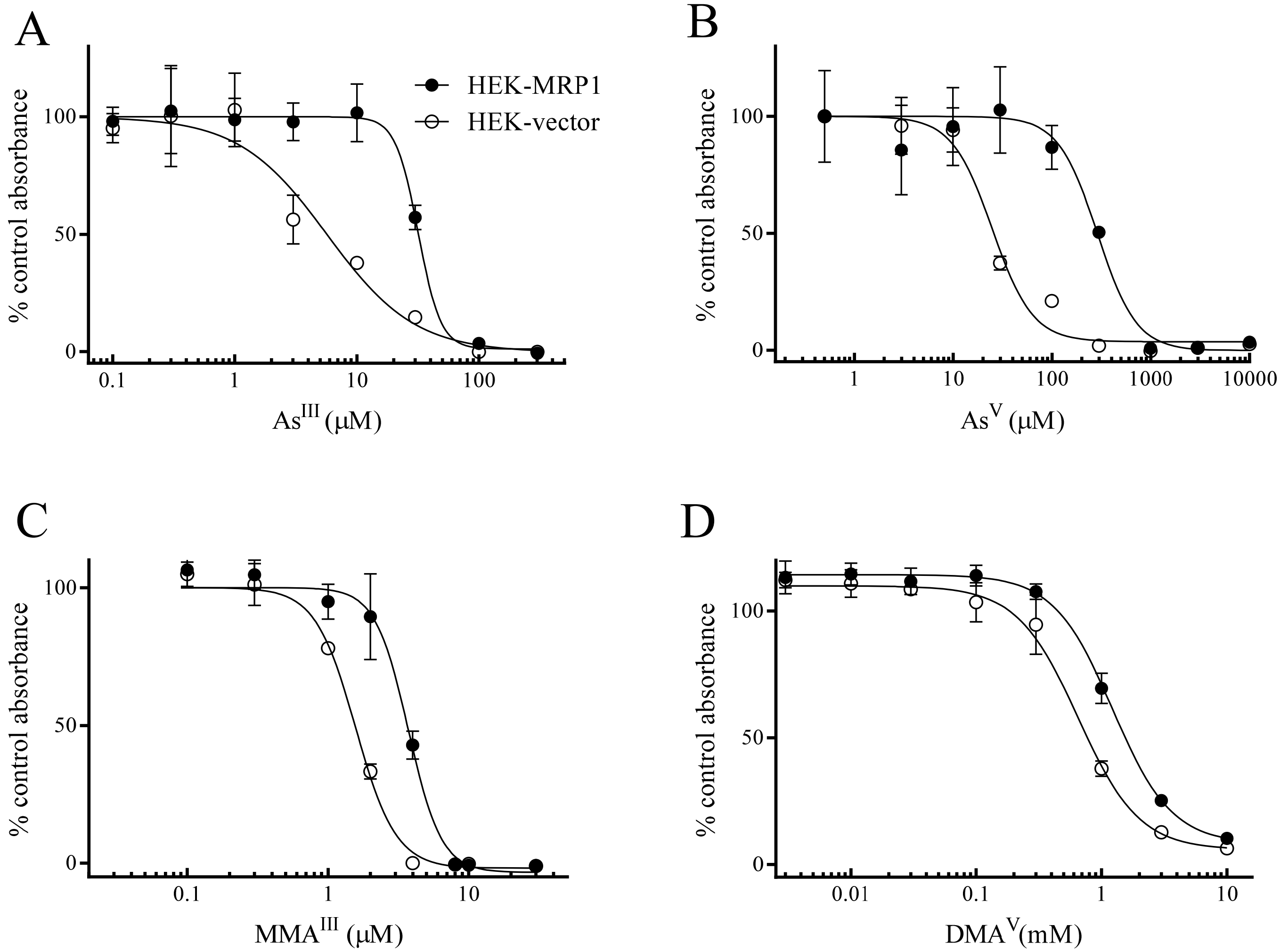

FIGURE 2 (Banerjee *et al.*)

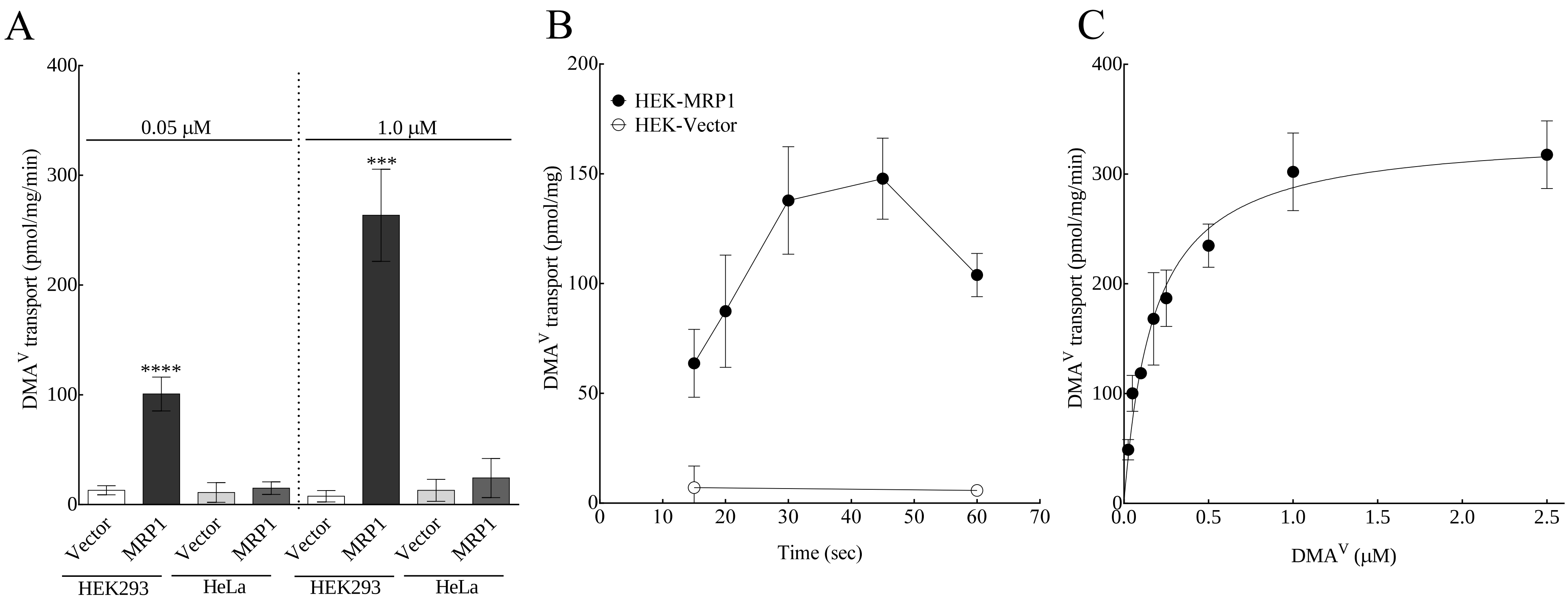

FIGURE 3 (Banerjee *et al.*)

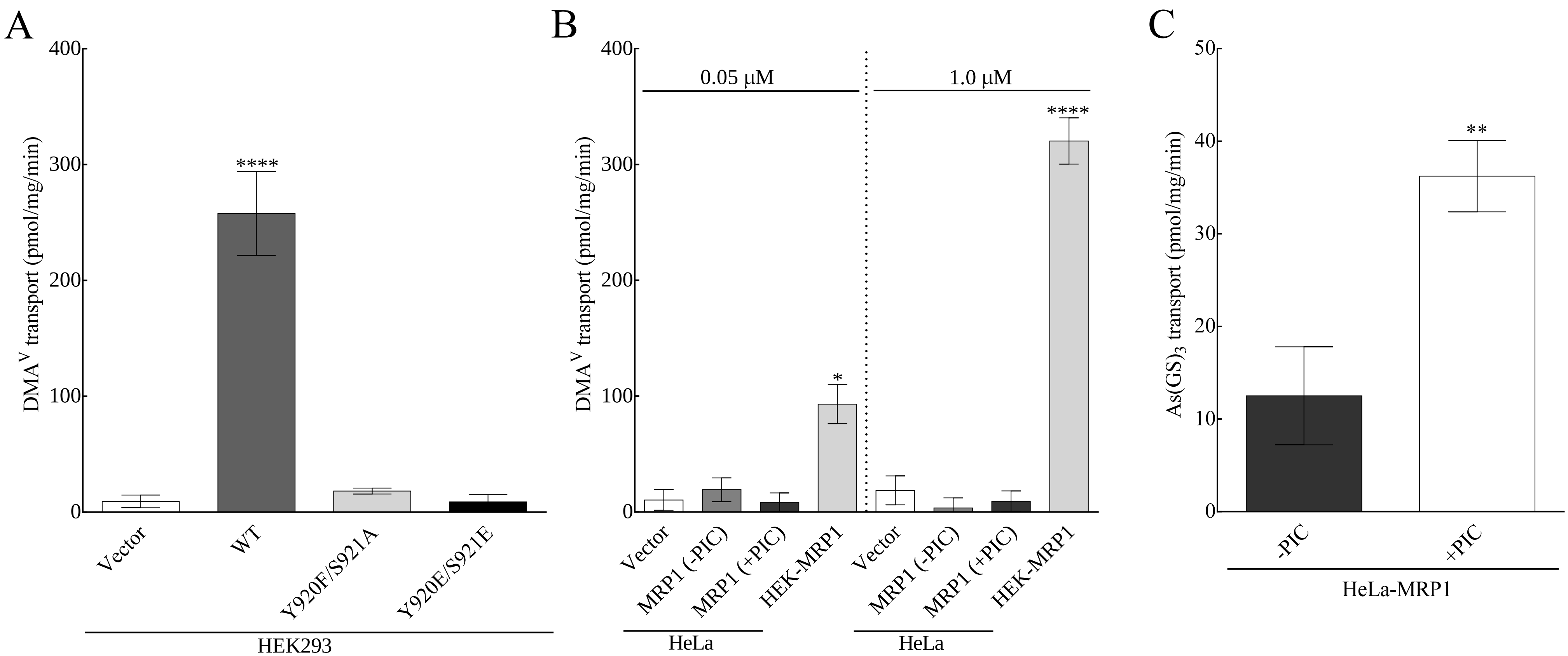

FIGURE 4 (Banerjee *et al.*)

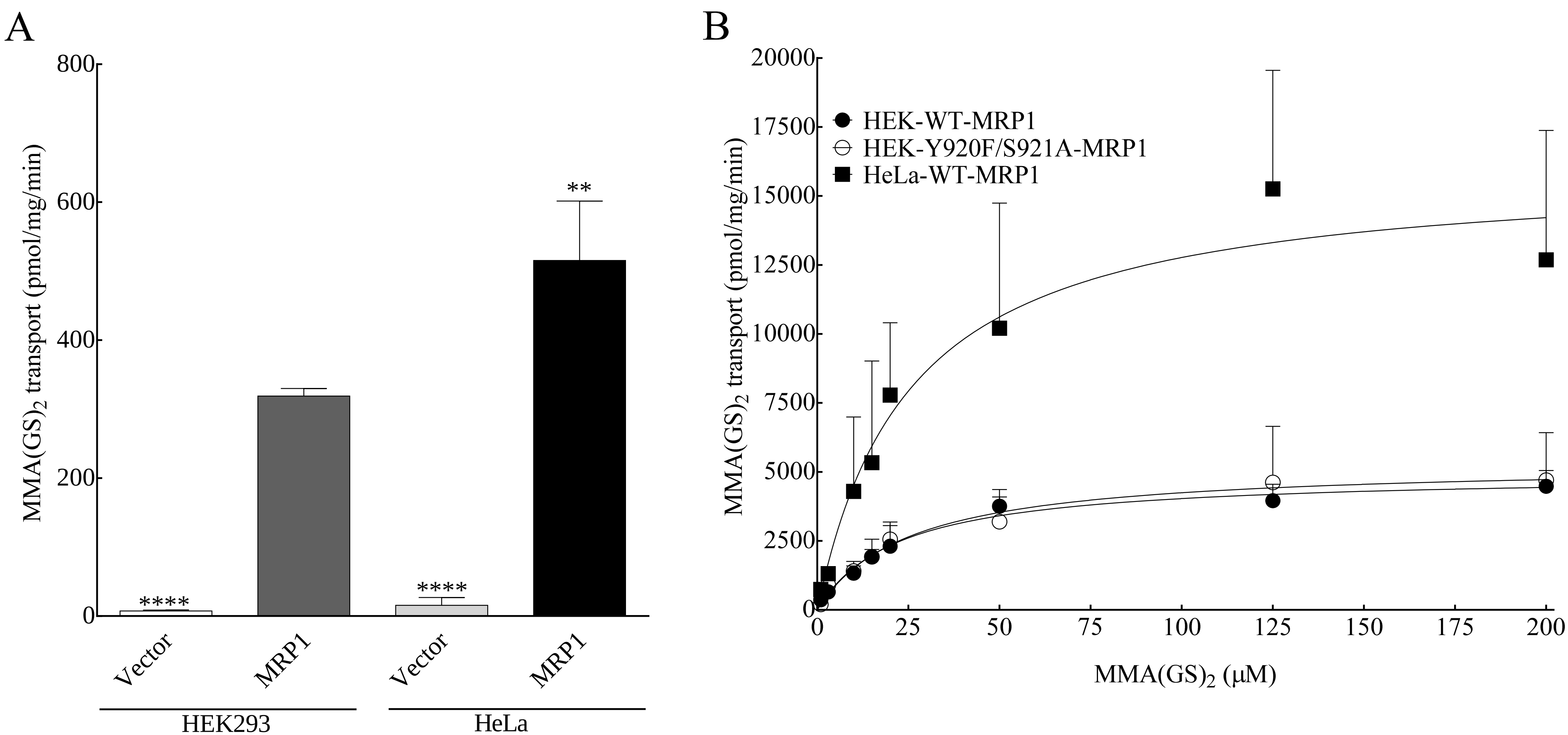

FIGURE 5 (Banerjee *et al.*)

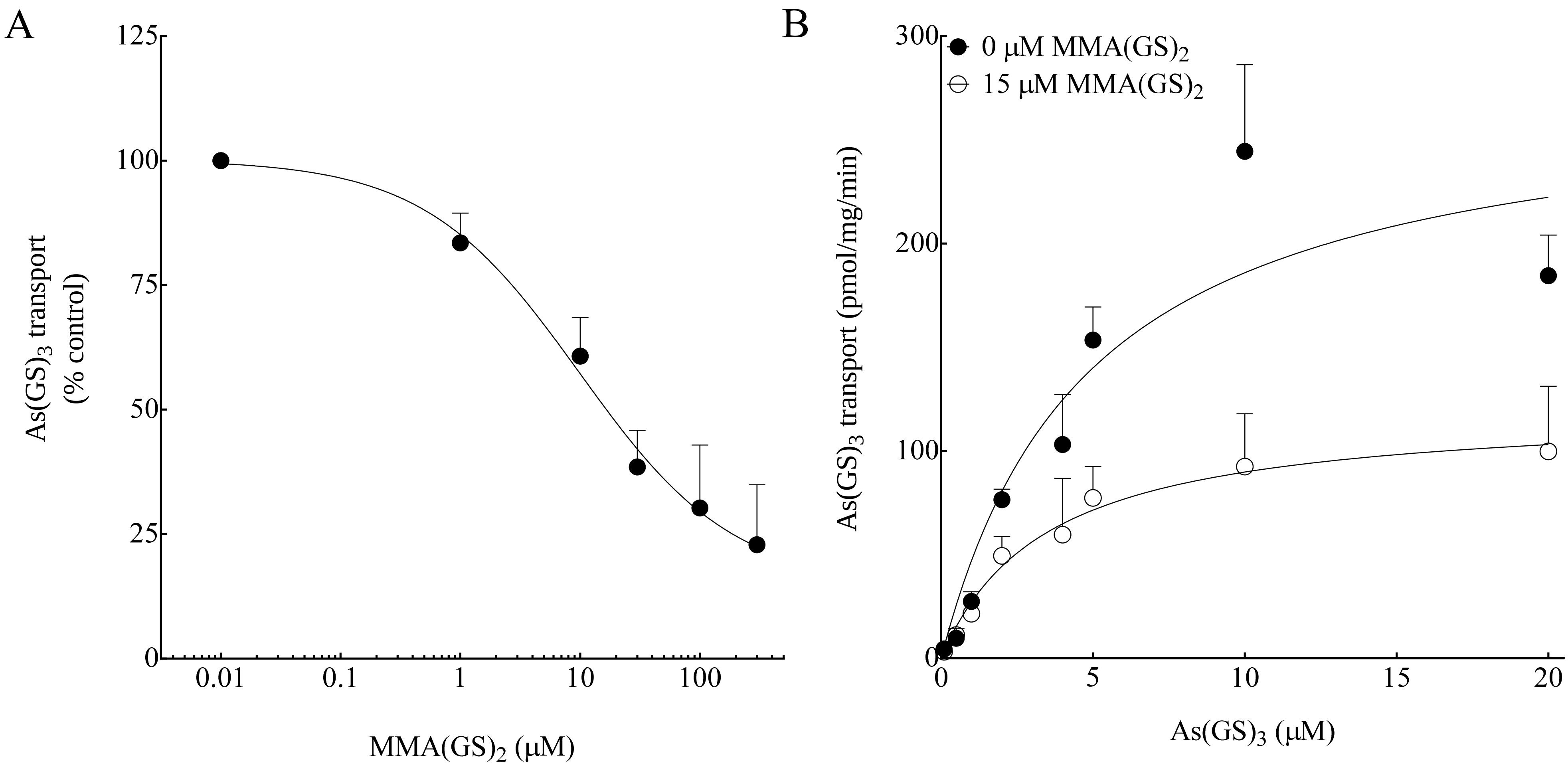

Drug Metabolism and Disposition

Supplemental Data

Multidrug Resistance Protein 1 (MRP1/*ABCC1*)-mediated detoxification and transport of methylated arsenic metabolites differs between human cell lines.

Mayukh Banerjee, Gurnit Kaur, Brayden D. Whitlock, Michael W. Carew, X. Chris Le, and Elaine M. Leslie

Supplemental Figure 1: Relative protein levels of MRP1 in membrane vesicles prepared from HeLa and HEK293T cells.

Supplemental Figure 2: Functional evaluation and protein levels of membrane vesicles prepared from HEK293T cells expressing MRP1-mutants.

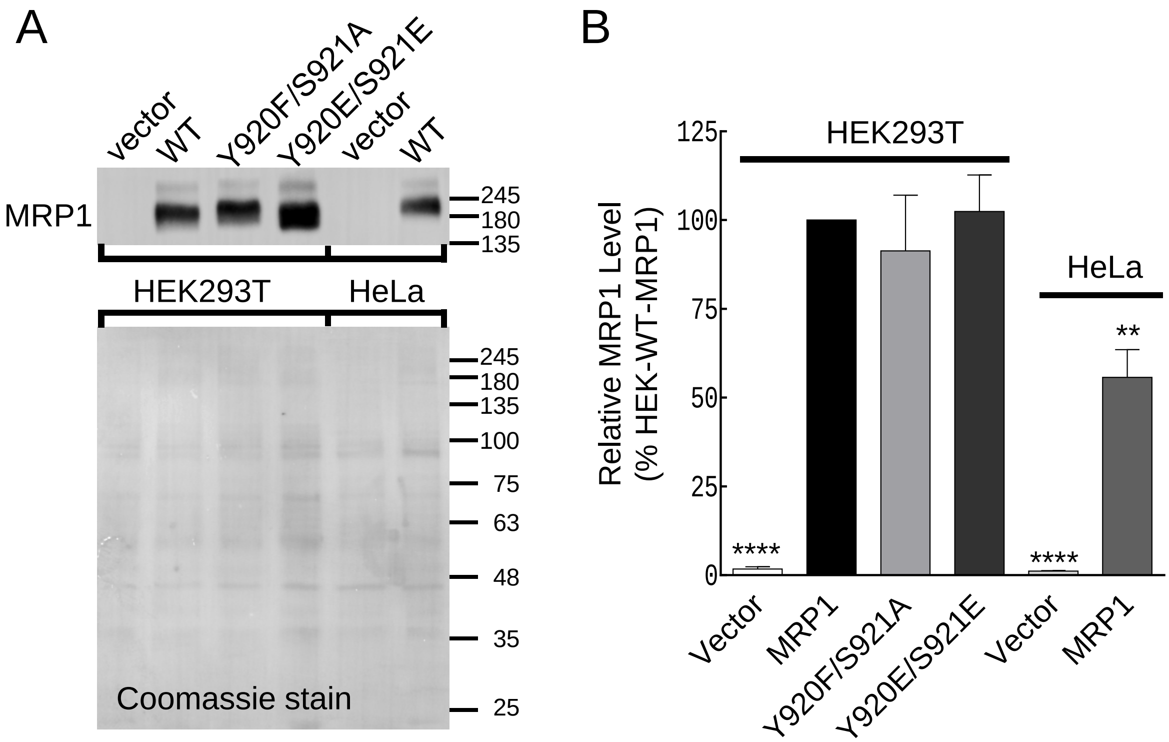

Supplemental Figure 1: Relative protein levels of MRP1 in membrane vesicles prepared from HeLa and HEK293T cells. (A) Membrane vesicles (0.5 µg protein per lane) prepared from HEK293T cells (transiently expressing empty pcDNA3.1 vector (vector), WT-, Y920F/S921A, or Y920E/S921E-MRP1) or HeLa cells (stably expressing vector or WT-MRP1) were resolved by 7% SDS-PAGE and immunoblotted with the MRP1-specifc MAb MRPr1 (1:10,000) (top panel). Blots were then stained with Coomassie blue for total protein levels (bottom panel). (B) Densitometry on the MRP1 and Coomassie stained blots was performed using ImageJ software. Vector control, WT- and mutant-MRP1 levels were normalized for protein loading as needed based on the entire corresponding lane of the Coomassie stained blot.and then plotted as a % HEK-WT-MRP1 level. Bars represent the mean (± S.D.) values obtained from three independent vesicle preparations. ** $p < 0.01$, ****$p < 0.0001$ (one way ANOVA followed by a Dunnett's multiple comparisons post hoc test).

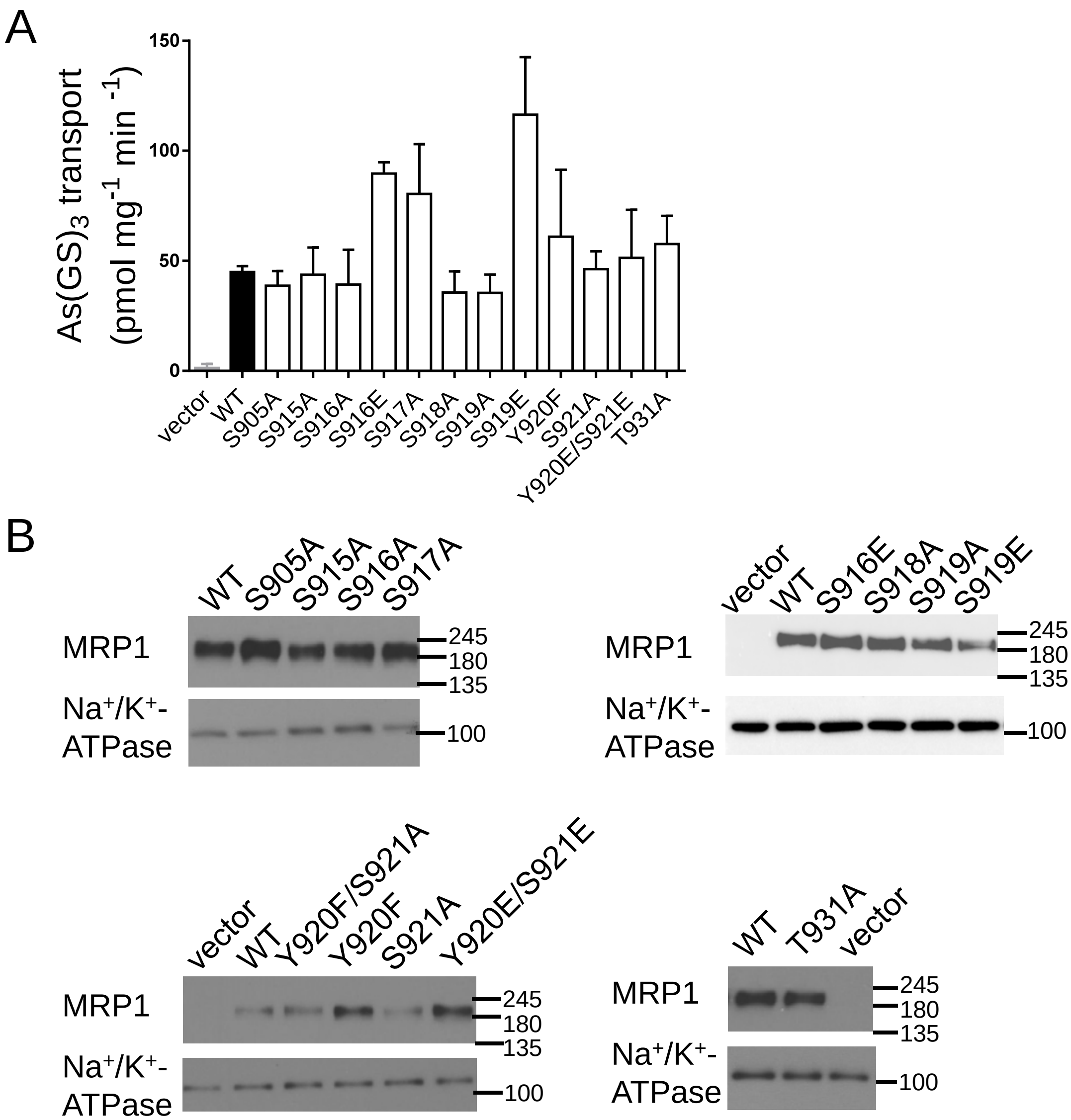

Supplemental Figure 2: Functional evaluation and protein levels of membrane vesicles prepared from HEK293T cells expressing MRP1-mutants. (A) ATP-dependent uptake of $As(GS)_3$ (1 μM, 40 nCi) by membrane vesicles (20 μg of protein) prepared from HEK293T cells expressing empty pcDNA3.1 vector (vector), wild-type MRP1 (WT), or potential MRP1 phosphorylation site mutant. Bars represent the mean (± S.D.) of a triplicate determination in a single experiment and are corrected for MRP1 level. Membrane vesicle preparations were identical to those used to characterize DMA^V transport by these mutants. (B) Membrane vesicles (0.5 µg protein per lane) prepared from HEK293T cells (transiently expressing empty pcDNA3.1 vector (vector), WT-, or mutant MRP1were resolved by 7% SDS-PAGE and immunoblotted with the MRP1-specifc MAb MRPr1 (1:10,000). Blots were then probed with the Na^+/K^+-ATPase-specific PAb H-300.